

Studying the Ultrafast Dynamics of the Insulator-Metal Transition in Single Crystal VO₂

Emily Chavez

University of Colorado, Boulder REU 2011

ABSTRACT

The focus of my research project this summer was towards the investigation of the insulator-metal transition dynamics of vanadium dioxide. A summary of the currently known, as well as debated, properties of the material is given here. Also given are the various experimental details involved in the measurements. We used femtosecond pulses in pump-probe experimentation to achieve time-resolved reflectivity measurements of single crystallite VO₂. Preliminary results are presented and the eventual undertakings of the experiment are discussed.

I. INTRODUCTION

Within the last few decades a wide variety of materials exhibiting unusual electronic properties due to electron-electron interactions have been discovered. Exciting effects such as high-temperature superconductivity, colossal magneto-resistance, and ferroelectricity are among a few such interesting behaviors discovered. Such unique electronic and magnetic effects are all amongst a class of materials featuring strongly correlated electron interactions.

Conventional materials such as classical insulators and metals can be described through simple models following basic band-theory and the approximation of non-interacting between electrons. A strongly correlated material, however, must rely on more complicated models that account for the interaction of electrons with each other. Understanding the exotic dynamics present within strongly correlated materials often requires extreme environments for experimentation, such as ultra-low temperatures, both very high and very low pressures, and high magnetic fields, as well as the use of precision tools such as ultrafast laser probes, high spatial resolution microscopies, and various spectroscopic methods (photoelectr-

on, TERS, X-ray diffraction, etc.).

This summer was spent studying the correlated electron phenomena present within the transition metal oxide, vanadium dioxide (VO₂). This crystalline material undergoes a first-order transition from an insulator to a metal upon thermal, optical, or electrical excitation. The rapid transition, along with distinct changes in crystal symmetry and electrical properties, has surrounded VO₂ with much attention in the scientific community. The on-going effort towards understanding the dynamics of this material is one employing the far-reaches of experimental physics, rousing debate among scientists for decades, and exciting the imagination for innovative new technologies.

By uncovering more of the fine scale structural and electronic changes occurring within the transition regime we come closer to effectively modeling the material systems. Eventually this may launch VO₂ into a wide range of applications many of which already have promising outlooks. These include high-speed digital optical computing, electrical and optical switches, temperature and pressure sensors, infrared

coatings, energy-efficient windows, photonic crystals, and many others [1-4].

II. BACKGROUND ON VO₂

The metal-to-insulator transition (MIT) of vanadium dioxide, first detailed by F.J. Morin in 1959, has been cause to much excitement in the past several decades. The first-order transition occurs thermally at a temperature of $\sim 68^\circ\text{C}$, which so near to room temperature, adds increased appeal to the potential applications of both VO₂ thin films and single crystallites. The MIT can also be induced by photo-excitation, as in the pump-probe experiment described later on.

The MIT displays a change in lattice symmetries, from the distorted rutile structures of the insulating phase to a purely rutile (tetragonal) metallic structure (Fig. 1a). There are two models for the driving mechanism of the MIT. The Peierls model describes a structural instability in the higher symmetry rutile phase and hence the dimerization of the V-atoms is energetically favorable. The pairing of V-atoms implies a doubling of the lattice periodicity, which leads to the opening of an insulating band-gap. [5] To put otherwise, the band-like Peierls mod-

el relies on evidence for electron-phonon interactions within the transition. The competing Mott-Hubbard model finds that the insulating phase is stable due to strong Coulomb repulsions. The metallic state is therefore only possible when there is enough energy in the system to overcome the electron-hole attractions, therefore allowing sufficient free carriers for conduction. Or in other words, the transition in the Mott-Hubbard case is driven by strongly correlated electron interactions [6,7]. Although there are still efforts to settle this debate towards one model or another, the large amount of evidence for each has directed new theory where both Peierls and Mott-Hubbard models are active mechanisms within the transition [8]. Accurately modeling the transition dynamics is still of critical interest within current VO₂ research for the advantages such a model will have in the design of technological devices as well as for explaining the curious physics involved in the MIT on a fundamental level.

However, settling this debate gets only more problematical as we uncover further information regarding the complexities of VO₂'s crystallographic phases. VO₂ is stable as an insulator at room temperature, however its insulating phase can exist in any

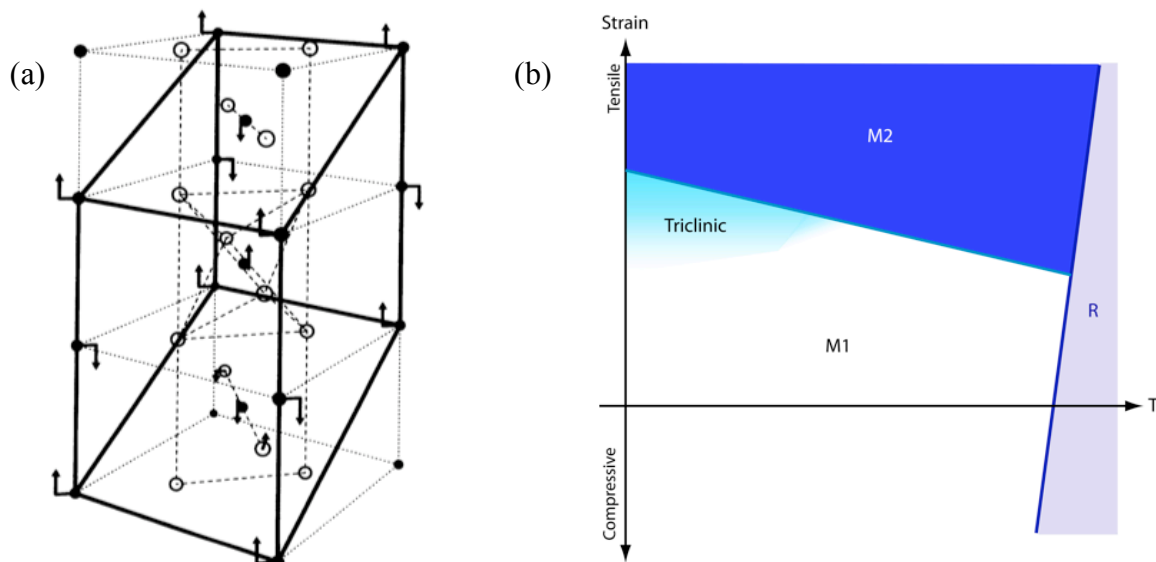


FIG 1. (a) Monoclinic (solid) and tetragonal (dotted) crystal structures of VO₂. Arrows indicate distortions from metallic to insulating. [10] (b) Phase diagram showing temperature versus strain dependence of VO₂ [16]

of three different crystallographic symmetries: the monoclinic M_1 or M_2 structures, or the triclinic T structure. Differing strain within the samples, which can result from the growth process, determines the symmetry of the stable phase for single crystallites and also can lead to inhomogeneous domain formation upon excitation within thin films. Depending on the inherent or applied strain, differing transition temperatures are observed [9] also possibly differing transition times. Temperature and strain dependence can be seen in the phase diagram presented in Figure 1b. Once excited from the insulating to the metallic phase, VO_2 experiences a strong increase in conductivity and large changes in reflectivity [10], which is of great appeal for its use in electronic and optoelectronic applications. Making use of VO_2 in device application, however, will require predictable phase behaviors along with some level of domain control, which is not possible in the polycrystalline thin films commonly studied.

Previous time-resolved studies of the MIT have primarily focused on polycrystalline thin films, besides a study done by Lysenko et al. on thin films of pure M_1 phase [11]. However, no studies have yet been done to resolve the ultrafast transition of single phase crystallites. The high elasticity, homogeneity, and distinct orientation of single crystal nano-beams and micro-structures makes them ideal for strain engineered devices [12] and other nanotechnologies. Here we have conducted femtosecond pump-probe experiments on single crystal micro-structures of varying phase and orientation. We characterized the samples using Raman spectroscopy and resolved phonon modes within time-resolved measurements of the MIT to compare with observed Raman peaks. We were able to resolve excitation and relaxation times for the photo-induced transition.

III. EXPERIMENTAL DETAILS

Single crystalline VO_2 micro-rods and platelets were grown using vapor phase transport deposition (VPT) onto a SiO_2 substrate. [13] Micro-rods average in size from a few microns in length and 100's of nanometers in width and depth. Platelets average several microns in length and width. These micro-structures are characterized using time-resolved Raman spectroscopy. 632.8nm HeNe laser light is used to illuminate a sample structure through a 50x Olympus objective in dark field. Back-scattered light is collected through the same objective and sent through a 632nm Raman filter and into a spectrometer. Through the inelastic scattering of light off the crystal lattice we can resolve Raman modes within the spectra detailing the lattice structure of the single-phase crystals. By fitting the Raman mode peaks with a Lorentzian function we were able to determine accurate peak positions. In particular the $\sim 610 \text{ cm}^{-1}$ peak is characteristic in determining the insulating phase structure [10]. Here we have determined platelet type crystals of monoclinic M_1 and M_2 phase, as well triclinic T phase for use in pump-probe experimentation. In contrast, previous pump-probe experiments have typically used polycrystalline VO_2 thin films, where a single crystal phase and orientation cannot be resolved. [11,14]

The pump-probe set-up employs 800nm light from a Verdi pumped Ti:Sapphire laser manufactured by KMLabs. Pulses are generated through passive mode-locking within the Ti:Sapphire optical cavity. The pulse energies from the Ti:Sapphire oscillator alone are not sufficient for many of the experiments performed in our lab. Therefore the pulses are amplified by passing through a regenerative amplifier. The regenerative amplifier operates by first passing the pulse through a grism pair to induce a negative chirp, i.e. the pulse starts at higher frequencies and ends at lower. The

temporal lengthening of the chirped pulse acts to ensure safe amplification in which the gain medium is not damaged and the pulse profile is preserved. The pulse is amplified in a cavity, again with a Ti:Sapphire gain medium, pumped with 532nm Verdi light. A Pockels cell controls the pulse repetition within the cavity. For our experiments we operate at a repetition rate of 125kHz. Once amplified, the pulse is sent through a glass block to compensate for the negative chirp. We can achieve short pulses of energy up to 10 μ J and lengths of 45fs. Short pulses of this time scale are essential to effectively resolve the MIT, as the transition can occur in as fast as \sim 80 fs [15].

To characterize these short pulses we used a technique called *second harmonic generation frequency-resolved optical gating* (SHG-FROG). The basis of this approach is to overlap the pulse with itself in a nonlinear optical medium, in this case a BBO crystal. This auto-correlation is then spectrally resolved via spectrometer. Both pulse shape and phase can be extracted from this method, which explains its advantage over other autocorrelation methods. By using an iterative algorithm, the length of the pulse can be extracted from the fitted frog trace. Figure 2 shows a typical FROG trace of our system. Optimizing the pulses can be achieved by tuning the distance and angle between the grism pair, in order to compensate for second- and third-order dispersion respectively.

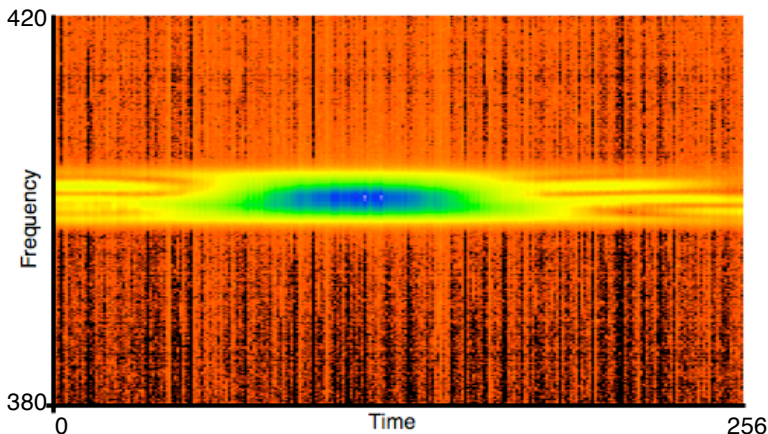


FIG 2. Typical FROG trace of a short laser pulse graphed as time in fs versus frequency in μ (nm). The wings on either side result from third-order dispersion.

Once short pulses of \sim 45fs have been achieved, we direct the pulses into our set-up for pump-probe experimentation. A schematic of this set-up is shown in Figure 3. We split the beam with a 5%-95% beam splitter, 5% beam intensity becoming the probe arm and 95% the pump arm. Light from the laser is linearly polarized. Through the use of an optical periscope the polarization of the probe arm is made to be oriented perpendicularly with respect to the pump arm. Before entering the detector, a New Focus DC photodiode, the signal is sent through a linear thin film polarizer to filter any residual light from the pump beam out of the probe signal. This is essential for optimizing the signal/noise ratio.

To further increase the signal-to-noise ratio, an optical chopper was employed before focusing onto the sample. The chopper has a series of apertures on both an inner and outer rim which function to modulate two beams at separate frequencies. Here the pump is chopped at 707 Hz while the probe is chopped at 505 Hz. We then set a Zurich lock-in amplifier at the difference frequency between the two (202 Hz), which yields a significantly clearer signal as it selects for the magnitude of the pump induced change in the probe signal.

The pump and probe beams are focused onto the sample by a parabolic mirror. The sample and beam focus can be imaged separately by using either a white light source or the laser beams to illuminate the sample and directing the reflected image into a CCD. By imaging a topographical sample of evenly spaced uniform structures with known size, the beam focus could be roughly approximated (\sim 20 μ m pump spot size and \sim 10 μ m probe spot size). A different technique for determining the focal size was also used in which a razor edge was passed through the beam path. Transmitted beam power vs. transverse position was measured.

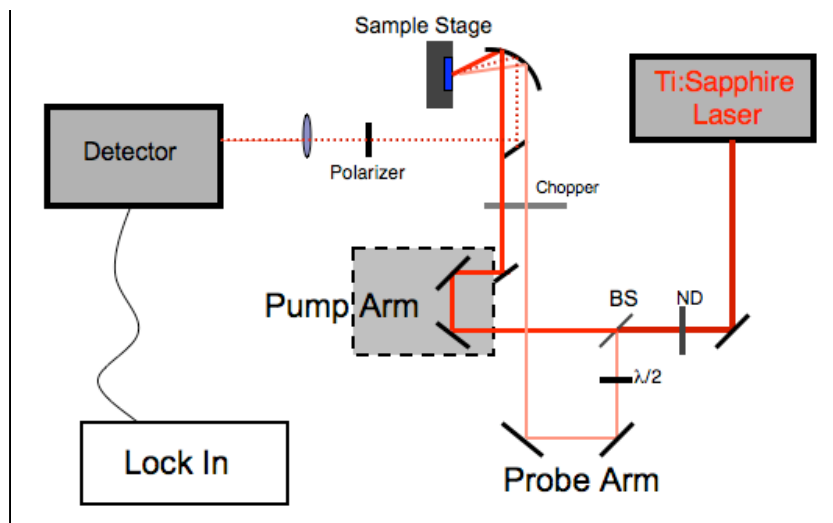


FIG. 3. Schematic of the pump-probe set-up

The resulting curves were fitted with an error function and then related to a Gaussian profile in which the full-width half-max of each beam could be determined. The results agreed reasonably with initial approximations; the pump focus was determined to be $\sim 15\mu\text{m}$ in width and the probe to be $\sim 8\mu\text{m}$ in width. The focus sizes of the pump and probe were needed to calculate the fluence incident on the micro-rods during experimentation. Using various neutral density filters in the pump arm, we could adjust the pump fluence between $1\text{-}20\text{mJ}/\text{cm}^2$.

The time-resolved reflectivity measurements are made possible by controlling the delay between pump and probe beams as they overlap on the sample. The pump beam is retroreflected from a linear motorized translation stage, which we scan in $1\mu\text{m}$ steps, corresponding to a 6.7 fs delay. As the pump beam excites the VO_2 crystallite, the probe beam can perturb the system chronologically through the excitation. This yields a delay vs. reflection curve of the transition. By adjusting the fluence accordingly it is possible to observe structurally characteristic phonon oscillations within the measured reflectivity.

IV. RESULTS AND DISCUSSION

Single crystal platelets were studied with Raman spectroscopy on a sample held at room temperature. Figure 4. shows a Ra

man spectrum of a VO_2 platelet labeled J (Shown in Fig. 5b) Spectra were taken both parallel to the length of the structure and perpendicular. Polarization dependence in several peaks was observed, as they emerged in one orientation but not the other. However, the characteristic peaks were reproducible between spectra. It was determined that all crystallites on this particular sample, along with structure J, were purely in the triclinic T phase. This was done by fitting the determining peak with a Lorentzian line-shape and comparing peak position, in Raman shift (cm^{-1}), with those of known spectra.

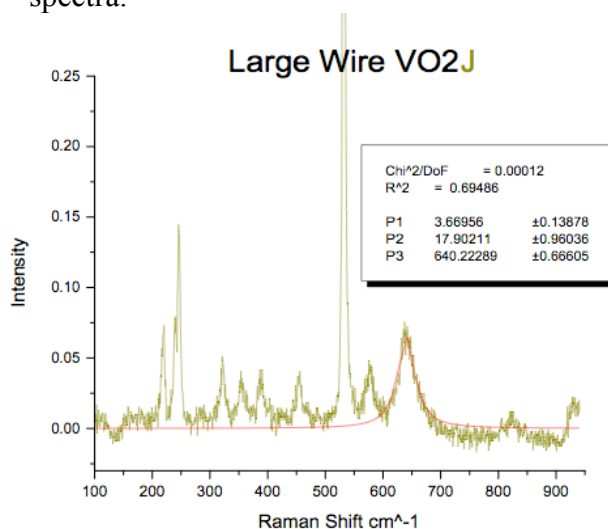


FIG. 4. Raman spectrum of sample platelet J with Lorentzian fit of the $\sim 640\text{ cm}^{-1}$ characteristic peak

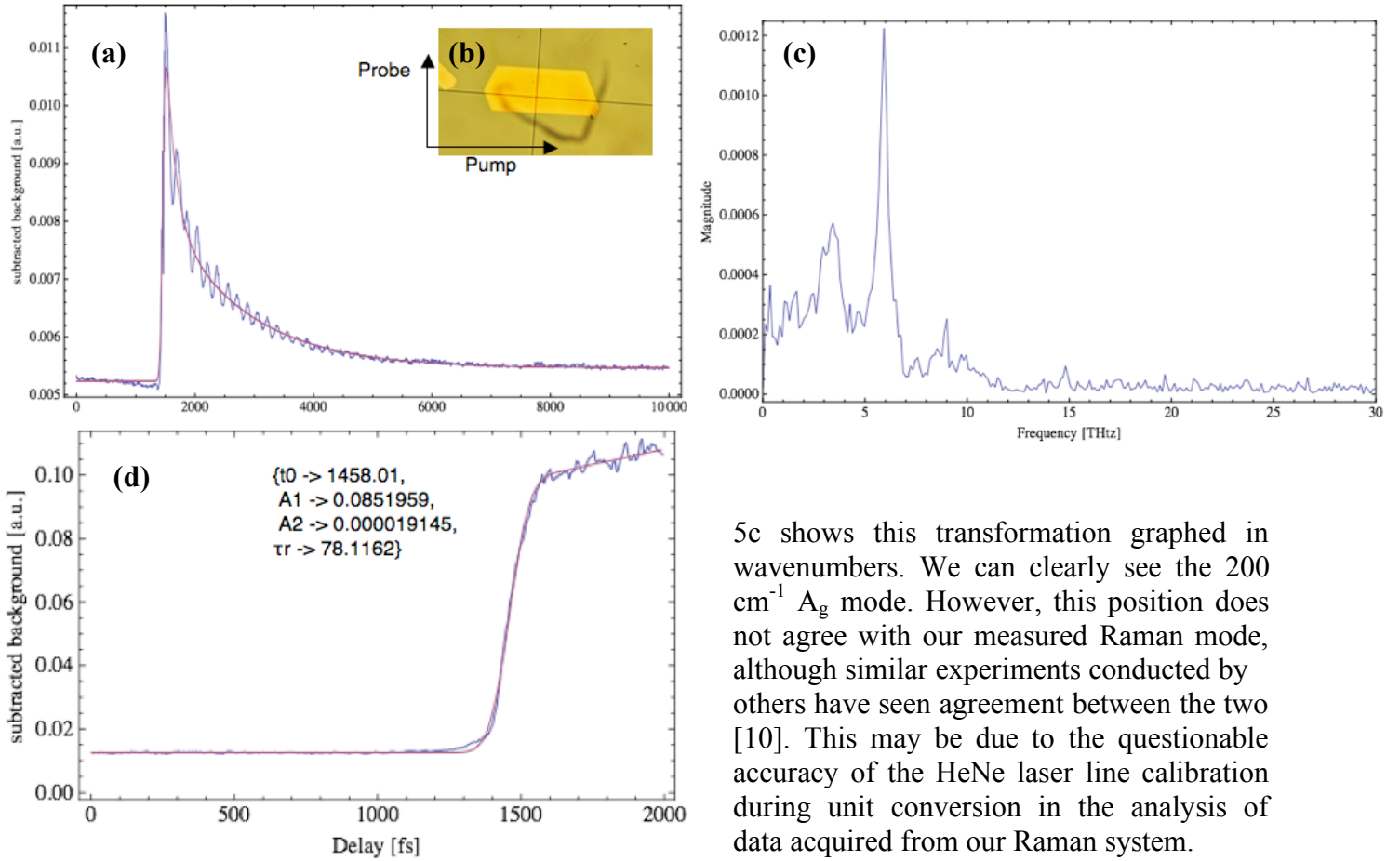


FIG. 5. (a) Transient reflection curve shown as pump-probe delay versus reflection intensity of VO₂ platelet J (shown as inset (b)). Polarization orientation with respect to the sample is shown. (c) The extracted phonon oscillations mapped in frequency space. (d) The transition region with fit and values shown

Transient reflectivity of the known structure was measured with a pump fluence of $\sim 2.4 \text{ mJ/cm}^2$ (Fig. 5a). Here we see a strong decrease in reflectivity upon pump/probe overlap followed by an exponential decay from electronic relaxation. The pump fluence used here allows observation of the rapid excitation through the transition regime and the immediate decay as the system relaxes back to its stable insulating state. The oscillations in reflectivity within the relaxation period are due to phonon oscillations within the crystal lattice. By first extracting the decay region and then taking a Fourier transform we were able to map these oscillations in the frequency domain. Figure

5c shows this transformation graphed in wavenumbers. We can clearly see the $200 \text{ cm}^{-1} A_g$ mode. However, this position does not agree with our measured Raman mode, although similar experiments conducted by others have seen agreement between the two [10]. This may be due to the questionable accuracy of the HeNe laser line calibration during unit conversion in the analysis of data acquired from our Raman system.

Figure 5d shows the transition region of a transient reflectivity measurement done on the same structure. The platelet was excited into the metallic phase with a strong pump fluence of 20 mJ/cm^2 . By fitting the curve with an error function, a time constant corresponding to the transition time was determined as $\sim 78 \text{ fs}$. Referring to the structural bottleneck observed by Cavalleri et al. [10], this transition time is near the supported minimum time required for the shift in crystal structure to occur.

The pump-probe experiment will continue by resolving transition dynamics of the remaining two monoclinic insulating phases, M_1 and M_2 . Single crystal structures of both phases will again be determined by Raman characterization. Then by comparing the transient reflection curves and resolved phonon oscillations of the three insulating types, we hope to determine any differences between transition and relaxation times, along with phonon peak shifts. These struc-

tures will also be subjected to controlled variations in polarization, excitation fluence, and possibly temperature and strain.

Experimentation with the photo-induced MIT in single crystalline VO₂ micro-structures has much promise in revealing the finest details of the much debated dynamics of this material. Further experimentation will hopefully lead towards effectively implementing VO₂ in a wide potential of applications.

ACKNOWLEDGEMENTS

I would like to sincerely thank Markus Raschke for making my research this summer possible and for all his support. A big thanks to Andrew Jones for his mentorship with this project throughout the summer. I also gratefully acknowledge Joanna Atkin for her everlasting patience and advice. Thanks to Molly May, a partner in crime. And many thanks to the REU coordinators, Leigh Dodd, Debbie Jin, and Dan Dessau for putting the program together.

REFERENCES

- [1] S. Pollack, D. Chang, F. Chudnovsky, et al. *J. Appl. Phys.* **78**, 3592 (1995)
- [2] G. Jorgenson and J. Lee *Sol. Energy Mater.* **14** 205 (1986)
- [3] O. Danilov and A. Sidorov, *Tech. Phys.* **44**, 1345 (1999)
- [4] A. Pevtov, D. Kurdyukov, V. Golubev, et al. *Phys. Rev. B.* **75** 153101 (2007)
- [5] L. Foglia *PHD Thesis Freie Universität Berlin* (2011)
- [6] H. Kim, Y. Lee, B. Kim, B. Chae, et al. *Phys. Rev. Lett.* **97**, 266401 (2006)
- [7] M. Qazilbash, M. Brehm, B. Chae, et al. *Science* **318**, 5857 (2007)
- [8] S. Biermann, A. Poteryaev, A. I. Lichtenstein, and A. Georges, *Phys. Rev. Lett.* **94**, 026404 (2005)
- [9] J. Atkin, S. Berweger, E. Chavez, and M. Raschke Submitted *Phys. Rev. Lett.* (2011)
- [10] C.N. Berglund and H.J. Guggenheim *Phys. Rev.* **185**, 1022, (1969)
- [11] S. Lysenko, A. Rua, V. Vikhnin, et al. *Phys. Rev. B.* **76** 035104 (2007)
- [12] J. Cao, E. Ertekin, V. Srinivasan, et al. *Nat. Nanotech.* **4** 732 (2009)
- [13] B.S. Gupton et al., *J. Am. Chem. Soc.*, **127**, 498-499 (2005)
- [14] C. Kubler, H. Ehrke, R. Huber, et al. *Phys. Rev. Lett.* **99**, 116401 (2007)
- [15] A. Cavalleri, T. Dekorsy, H. Chong, et al. *Phys. Rev. B* **70** 161102(R) (2004)
- [16] R. Wentzcovitch, W. Schultz, and P. Allen *Phys. Rev. Lett.* **72**, 21 (1994)

